Available online at www.sciencedirect.com

ScienceDirect

Mendeleev Commun., 2020, **30**, 276–278

Mendeleev Communications

Dehydrogenation of amine–boranes catalyzed by a $PC_{sp^3}P$ pincer iridium complex

Vladislava A. Kirkina,[a] Elena S. Osipova,[a] Oleg A. Filippov,[a] Gleb A. Silantyev,[a] Dmitri Gelman,[b] Elena S. Shubina[a] and Natalia V. Belkova*[a]

[a] *A. N. Nesmeyanov Institute of Organoelement Compounds, Russian Academy of Sciences, 119991 Moscow, Russian Federation. E-mail: nataliabelk@ineos.ac.ru*

[b] *Institute of Chemistry, The Hebrew University, Edmond Safra Campus, Givat Ram, 91904 Jerusalem, Israel*

DOI: 10.1016/j.mencom.2020.05.004

Dibenzobarrelene-based $PC_{sp^3}P$ pincer iridium complex bearing dangling CH_2OH groups, ($PC_{sp^3}P^{CH_2OH}$)IrH(Cl), catalyzes the dehydrogenation of amine–boranes at the reaction rate changing counter intuitively in the order: $Me_2NH{\cdot}BH_3$ > > $Bu^tNH_2{\cdot}BH_3$ > $NH_3{\cdot}BH_3$. The spectral (IR and NMR) data and DFT/M06 calculations have revealed that the binding of amine–boranes to the dangling OH group leads to an additional stabilization of the Ir···OH bond, thus hampering the dehydrogenation reaction, whereas the amine–borane coordination to iridium entails a *fac*- to *mer*-transformation of the complex and initiates the catalytic H_2 evolution.

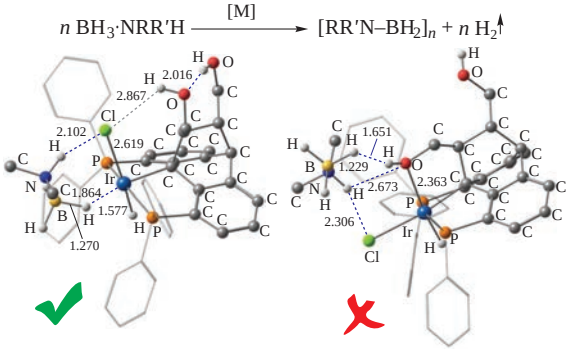

Keywords: iridium pincer complexes, catalytic dehydrogenation, amine–boranes, molecular spectroscopy, DFT calculations.

Amine–boranes, $RR'NH{\cdot}BH_3$, attract an attention of the researchers as compounds for the hydrogen storage systems owing to a theoretically high H_2 content[1,2] and also as promising objects for the design of BN ceramics and new polymeric materials, the so-called inorganic polymers.[3] These applications rely on the catalytic dehydrogenation of amine–boranes, so new catalytic studies keep appearing in the literature. A variety of recently developed (de)hydrogenation catalysts operate according to different metal–ligand cooperation mechanisms, and new 'non-innocent' ligands and their complexes are under ongoing investigations.[4–6] A reversible switching between the different coordination modes observed in these compounds have revealed new patterns of practical reactivity in the non-oxidative (*i.e.*, alternative to the conventional oxidative addition/reductive elimination sequence) activation and formation of polar and non-polar bonds. At this end, many of such systems contain stereochemically rigid pincer ligands and preserve their geometry during the catalytic cycles.

Dibenzobarrelene-based $PC_{sp^3}P$ pincer complexes of iridium have already been reported as efficient catalysts in the transfer (de)hydrogenation of polar and non-polar substrates.[7–11] Dibenzobarrelene-based $PC_{sp^3}P$ pincer iridium complex **1** is catalytically active in acceptorless dehydrogenation of alcohols (Scheme 1).

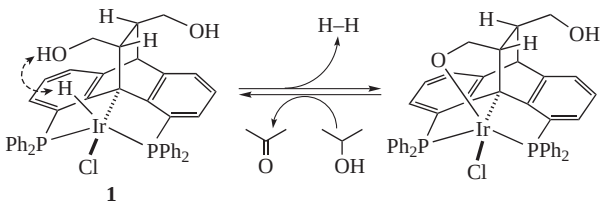

Scheme 1

The intramolecular interaction of iridium hydride ligand with the dangling CH_2OH group of **1**, which leads to a facile hydrogen release was hypothesized as the origin of its high catalytic activity.[12] Its catalytic performance is comparable to or even exceeds the state of the art catalysts operating under the neutral conditions.[13,14]

Among the benzene-based pincer Ir^{III} complexes, ($^{Bu^t}$POCOP)IrH_2 [$^{Bu^t}$POCOP is κ^3-2,6-(Bu^t_2P–O)$_2C_6H_3$] appeared to be highly efficient not only in the dehydrogenation of alkanes, but also in the dehydrogenation of $NH_3{\cdot}BH_3$.[15] Our works on related ($^{Bu^t}$PCP)IrH(Cl) and ($^{Bu^t}$PCN)IrH(Cl) ($^{Bu^t}$PCP is κ^3-2,6-($Bu^t_2PCH_2$)$_2C_6H_3$ and $^{Bu^t}$PCN is 1-{3-[(di-*tert*-butylphosphino)methyl]phenyl}-1*H*-pyrazole) have revealed an important influence of the steric properties of pincer ligand on the catalytic activity of this series of iridium hydrides and unveiled the dehydrogenation mechanism for amine–boranes.[16–18] The hydrogen NH···Cl bond and BH coordination to the iridium appeared to be important initial steps in the hydridochloride precatalyst activation [Figure 1(*a*)], whereas the dihydrogen NH···H–Ir bond and BH···Ir interaction [Figure 1(*b*)] initiate the hydride (from B–H to Ir) and proton (from NH to Ir–H) transfers in the catalytic cycle. In view of the different properties of sp^2 and sp^3 PCP scaffolds and the presence of dangling functional group in the latter, the present work was aimed at testing the catalytic activity of dibenzobarrelene-based $PC_{sp^3}P$ complex **1** in amine–boranes dehydrogenation.† Figure 1 shows the structures of considered intermediates.[16–18]

† All the manipulations were performed under an argon atmosphere using the standard Schlenk technique. The H_2 production during the reaction of amine–boranes with complex **1** was monitored by measuring the volume of hydrogen gas released. In a typical experiment, DMAB (8.8 mg, 0.246 mmol)

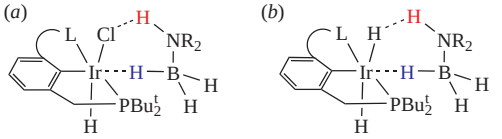

Figure 1 Structures of the key hexacoordinated intermediates in the (*a*) precatalyst activation and (*b*) catalytic cycle of DMAB dehydrogenation catalyzed by (PCL)IrH(Cl) complexes.

Volumetric tests demonstrated that *ca.* 1 mol% of complex **1** readily dehydrogenated amine–boranes yielding 0.6 equiv. of H_2 within 2–3 h at room temperature (Figure 2, Table S1, see Online Supplementary Materials), whereas 1 equiv. of H_2 could be obtained at prolonged reaction times (*e.g.*, in 6 h in the case of $Bu^tNH_2{\cdot}BH_3$). A higher degree of self-association in low-polar media[19] hampers the $Me_2NH{\cdot}BH_3$ (dimethylaminoborane, DMAB) dehydrogenation in C_6H_5F, where the reaction is slower ($k_{obs} = 3.9 \times 10^{-5}$ s^{-1}) than that in dimethoxyethane (DME) and CH_2Cl_2 ($k_{obs} = 1.8 \times 10^{-4}$ s^{-1}) (Figure S1). An analysis of the initial reaction rate for different DMAB and catalyst concentrations (Figure S2) revealed that the overall reaction obeys the first order law in both the components: $-d[DMAB]/dt = k_{obs}$ and $[DMAB] = k[\mathbf{1}][DMAB]$.

The structure of complex **1** differs from that of many other catalysts containing 'non-innocent' or bifunctional ligands, *i.e.*, the hydroxymethyl group is formally far away from the metal. Results of the variable temperature IR and NMR (^{1}H and ^{31}P) analysis for **1** and its analogue, the COOEt substituted complex, in different media (CH_2Cl_2, toluene, DMSO, and mixed solvents) in combination with the quantum chemical calculations (DFT/M06) have revealed a flexibility of the dibenzobarrelene-based scaffold[20] unprecedented for conventional pincer ligands. These complexes prefer the facial configuration of PCP ligand with P–Ir–P angle of *ca.* 100° (*fac*-isomers: *fac*-**1-I** and *fac*-**1-II**, Figure S3). Such geometries arise due to the stabilizing Ir···OH interaction and differ by the mutual arrangement of H and Cl ligands. The *fac*-isomers can be transformed into the meridional ones with almost linear P–Ir–P arrangement (*mer*-isomer: *mer*-**1**, see Figure S3) in the presence of coordinating additives (MeCN, DMSO, or pyridine).[20,21] In the case of **1**, this causes the shift of Ir–H stretching vibration band ν(IrH) in the IR spectra from 2038 to 2225 cm^{-1} and the appearance in ^{1}H NMR spectra of hydride triplet resonance at δ_H from –19 to –22 instead of the doublets of doublets at *ca.* –9 ppm.[20,21] Upon the addition of DMAB to the solution of **1** in CH_2Cl_2 at 275 K, several new bands appear in the IR spectra evidencing the DMAB coordination to iridium (Figure 3). The

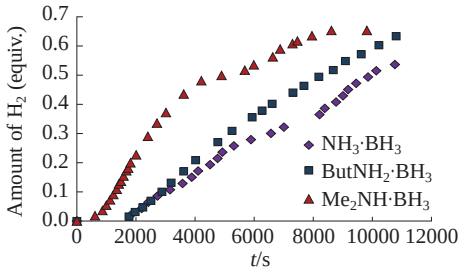

Figure 2 Kinetic curves for the H_2 evolution from amine–boranes ($c = 0.07$ mol dm^{-3}) in the presence of complex **1** (1.2 mol%) at 298 K in DME.

was dissolved in a solvent (3.0 ml) in a round-bottomed flask ($V = 10$ ml), and the flask was closed with a tight-fitting rubber septum. The required amount of **1** (dissolved in 0.5 ml of the same solvent) was transferred *via* syringe to the stirred amine–borane solution. Timing was started upon the catalyst injection. The hydrogen gas was collected in a water-filled, upturned burette through a Teflon tube. The volume of hydrogen gas collected was recorded periodically.

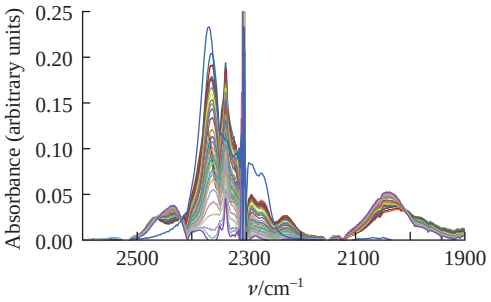

Figure 3 IR monitoring of the DMAB ($c = 0.01$ mol dm^{-3}) dehydrogenation in the presence of equimolar amount of complex **1** in CH_2Cl_2 at 275 K, $l = 0.01$ cm.

band at 2230 cm^{-1} was assigned to the ν(IrH) band in this new complex **1**·DMAB (Scheme 2). Its position is similar to the bands of hexacoordinated adducts of **1** with bases possessing the *mer*-configuration of dibenzobarrelene ligand.[20,21] In a similar way, a new ν(IrH) band at 2205 cm^{-1} appears in the IR spectra in the presence of $Me_3N{\cdot}BH_3$ (TMAB) at low temperatures (Figure S5). The DFT/M06 calculations have revealed the stronger binding of DMAB relative to TMAB ($\Delta G_{298} = -11.7$ and -4.0 kcal mol^{-1}, respectively) and predicted a lower frequency of $\nu(BH_{bridge})$ in **1**·DMAB as compared to that in **1**·TMAB, which appears close to the ν(IrH) band of **1**·DMAB (Figure S4, Table S2).

The amine–borane coordination to iridium also causes the appearance of new ν(BH) bands in the IR spectra. A higher frequency band at 2474 cm^{-1} was assigned to the stretching vibration of terminal (non-bonded) B–H bond in **1**·DMAB, whereas the stretching vibration of bridging BH group seems to be overlapped with the ν(IrH) band of the starting iridium complex, resulting in the wide band with its maximum at 2010 cm^{-1} (see Figure 3). The sharp intense ν(BH) band at 2338 cm^{-1} is typical of dihydrogen bonded BH moiety[19] and suggests an amine–borane interaction with the dangling OH group (see Scheme 2). This type of dihydrogen bonded complexes leads to the significant increase of oxygen nucleophilicity (due to the increase of negative charge) and consequently, to a stronger Ir···OH interaction as was confirmed by the DFT calculations (Figure S4). Such complexes should be more stable in the case of $Bu^tNH_2{\cdot}BH_3$ and $NH_3{\cdot}BH_3$, which is a possible reason for the lower reaction rate and noticeable induction period for the dehydrogenation of these amine–boranes (see Figure 2).

^{1}H NMR measurements have confirmed the formation of hexacoordinated *mer*-complex upon the DMAB addition to **1**. At low temperatures (200–250 K), a new triplet appears in the high-field region at δ(IrH) –23.15 ($^2J_{P-H}$ 12 Hz). When the H_2

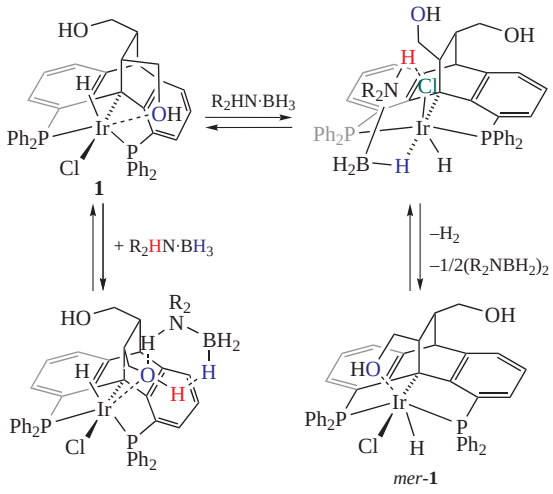

Scheme 2 Transformations of complex **1** in the presence of amine–boranes.

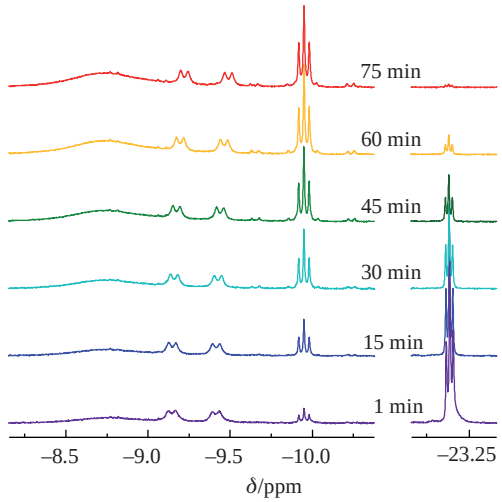

Figure 4 ^{1}H NMR monitoring of the DMAB dehydrogenation in the presence of complex **1** (1 equiv.) in CD_2Cl_2 at 272.5 K.

evolution begins above 250 K, this signal is gradually transformed into the yet another triplet at –9.95 ppm ($^{2}J_{P–H}$ 19 Hz, Figure 4). This suggests that the remaining iridium hydride catalyst preserves the *mer*-configuration of ligand, but is formally pentacoordinated (*mer*-**1**, see Scheme 2).[20,21] There are another two hydride resonances in the spectra, which appear upon the mixing and transform one into another during the reaction. They are broad signals at –2.1 and –8.6 ppm (Figure S6), which belong to complexes **1**·DMAB and **1**·(H_2B·NMe_2), respectively.[16–18,22] Complex *mer*-**1** remains catalytically active, so the addition of new portion of DMAB to the reaction mixture after the first run initiates another dehydrogenation cycle, which proceeds at the same rate (Figure S7).

In conclusion, the peculiarities of complex **1**, which promote dehydrogenation of alcohols, also lead to its decreased efficiency in the dehydrogenation of amine–boranes. The salient bifunctionality of amine–boranes results in their binding to the dangling OH group, thus providing the additional stabilization to the Ir···OH bond. That, in turn, hampers the BH coordination to iridium, necessary for the dehydrogenation to proceed. This explains the unexpected decrease in the reaction rate on going from $Me_2NH·BH_3$ to $Bu^tNH_2·BH_3$ and $NH_3·BH_3$.

This work was supported by the Russian Science Foundation (grant no. 19-13-00459). NMR spectroscopic data were acquired using the equipment of Center for Molecular Composition Studies at the A. N. Nesmeyanov Institute of Organoelement Compounds of the Russian Academy of Sciences with the financial support from the Ministry of Science and Higher Education of the Russian Federation.

Online Supplementary Materials

Supplementary data associated with this article can be found in the online version at doi: 10.1016/j.mencom.2020.05.004.

References

1 *Handbook of Hydrogen Energy*, 1st edn., eds. S. A. Sherif, D. Y. Goswami, E. K. (Lee) Stefanakos and A. Steinfeld, CRC Press, 2014.
2 L. H. Jepsen, M. B. Ley, Y.-S. Lee, Y. W. Cho, M. Dornheim, J. O. Jensen, Y. Filinchuk, J. E. Jørgensen, F. Besenbacher and T. R. Jensen, *Mater. Today*, 2014, **17**, 129.
3 A. A. Semenova, A. B. Tarasov and E. A. Goodilin, *Mendeleev Commun.*, 2019, **29**, 479.
4 D. Gelman and S. Musa, *ACS Catal.*, 2012, **2**, 2456.
5 J. R. Khusnutdinova and D. Milstein, *Angew. Chem., Int. Ed.*, 2015, **54**, 12236.
6 L. Alig, M. Fritz and S. Schneider, *Chem. Rev.*, 2019, **119**, 2681.
7 D. Gelman and R. Romm, *Top. Organomet. Chem.*, 2013, **40**, 289.
8 S. Musa, O. A. Filippov, N. V. Belkova, E. S. Shubina, G. A. Silantyev, L. Ackermann and D. Gelman, *Chem. Eur. J.*, 2013, **19**, 16906.
9 S. Musa, A. Ghosh, L. Vaccaro, L. Ackermann and D. Gelman, *Adv. Synth. Catal.*, 2015, **357**, 2351.
10 S. Cohen, A. N. Bilyachenko and D. Gelman, *Eur. J. Inorg. Chem.*, 2019, 3203.
11 S. Mujahed, F. Valentini, S. Cohen, L. Vaccaro and D. Gelman, *ChemSusChem*, 2019, **12**, 4693.
12 S. Musa, I. Shaposhnikov, S. Cohen and D. Gelman, *Angew. Chem., Int. Ed.*, 2011, **50**, 3533.
13 A. Friedrich and S. Schneider, *ChemCatChem*, 2009, **1**, 72.
14 G. E. Dobereiner and R. H. Crabtree, *Chem. Rev.*, 2010, **110**, 681.
15 M. C. Denney, V. Pons, T. J. Hebden, D. M. Heinekey and K. I. Goldberg, *J. Am. Chem. Soc.*, 2006, **128**, 12048.
16 L. Luconi, E. S. Osipova, G. Giambastiani, M. Peruzzini, A. Rossin, N. V. Belkova, O. A. Filippov, E. M. Titova, A. A. Pavlov and E. S. Shubina, *Organometallics*, 2018, **37**, 3142.
17 E. M. Titova, E. S. Osipova, A. A. Pavlov, O. A. Filippov, S. V. Safronov, E. S. Shubina and N. V. Belkova, *ACS Catal.*, 2017, **7**, 2325.
18 E. S. Osipova, O. A. Filippov, E. S. Shubina and N. V. Belkova, *Mendeleev Commun.*, 2019, **29**, 121.
19 I. E. Golub, E. S. Gulyaeva, O. A. Filippov, V. P. Dyadchenko, N. V. Belkova, L. M. Epstein, D. E. Arkhipov and E. S. Shubina, *J. Phys. Chem. A*, 2015, **119**, 3853.
20 G. A. Silantyev, O. A. Filippov, S. Musa, D. Gelman, N. V. Belkova, K. Weisz, L. M. Epstein and E. S. Shubina, *Organometallics*, 2014, **33**, 5964.
21 G. A. Silantyev, E. M. Titova, O. A. Filippov, E. I. Gutsul, D. Gelman and N. V. Belkova, *Russ. Chem. Bull., Int. Ed.*, 2015, **64**, 2806 (*Izv. Akad. Nauk, Ser. Khim.*, 2015, 2806).
22 C. J. Stevens, R. Dallanegra, A. B. Chaplin, A. S. Weller, S. A. Macgregor, B. Ward, D. McKay, G. Alcaraz and S. Sabo-Etienne, *Chem. – Eur. J.*, 2011, **17**, 3011.

Received: 6th December 2019; Com. 19/6081